Talanta 134 (2015) 712–717

Contents lists available at ScienceDirect

Talanta

journal homepage: www.elsevier.com/locate/talanta

Colorimetric detection of hydrogen peroxide and glucose using the magnetic mesoporous silica nanoparticles

Yonghong Wang [a,b], Bo Zhou [a], Shun Wu [a], Kemin Wang [b,*], Xiaoxiao He [b]

[a] College of Life Science and technology, Central South University of Forestry and Technology, 410004 Changsha, China
[b] State Key Laboratory of Chemo/Biosensing and Chemometrics, College of Biology, College of Chemistry and Chemical Engineering, Hunan University, Changsha 410082, China

ARTICLE INFO

Article history:
Received 3 October 2014
Received in revised form
8 December 2014
Accepted 11 December 2014
Available online 19 December 2014

Keywords:
Magnetic mesoporous nanoparticles
Peroxidase-mimic activity
Glucose
Detection

ABSTRACT

In this work, we synthesized a type of magnetic mesoporous silica nanoparticle (denoted as Fe_3O_4@MSN) with Fe_3O_4 as the core and mesoporous silica the shell. The superparamagnetic Fe_3O_4-core provides high peroxidase-mimic activity and makes the artificial enzymatic system easily recyclable. Furthermore, Fe_3O_4 nanoparticles are encapsulated in MSN shells to hinder the aggregation and keep them stable even under harsh conditions. Meanwhile, small active molecules are allowed to diffuse in and out of the MSN shells. Based on these functional units, the Fe_3O_4@MSN as robust nanoreactors can catalyze a self-organized cascade reaction, which includes oxidation of glucose by oxygen to yield gluconic acid and H_2O_2, and the latter further oxidizes 3,3,5,5-tetramethylbenzidine (TMB) to produce a color change. The Fe_3O_4@MSN, whose catalytic efficiency was not strongly dependent on pH and temperature, was successfully used for the detection of glucose and showed excellent sensitivity with a detection limit of 0.4×10^{-5} mol/L. Nevertheless, the assay is also highly selective toward the glucose detection.

1. Introduction

Nanomaterials have received considerable attention over the past few decades because of their unique size, shape, composition and structure-dependent properties. There has been an explosive growth in the use of nanomaterials as catalysts involving both homogeneous and heterogeneous catalysis. But the possibility of nanomaterials as certain artificial enzymes, important subdivisions of catalysis, had long remained unknown. Until the first nanoparticle-based artificial enzyme was reported, Fe_3O_4 nanoparticles were found to possess an intrinsic peroxidase-like activity [1], since which time some other nanomaterials have been evaluated as peroxidase mimetics. These studies show that the nanomaterial-based peroxidase mimetics enjoy advantages of low cost, high stability and tunability in catalytic activities and can be potentially used in bioassays and medical diagnostics.

Various nanomaterials including Fe_3O_4 magnetic nanoparticles [2,3], positively charged gold nanoparticles [4], cupric oxide nanoparticles [5], CuS nanoparticles [6], ceria nanoparticles [7,8], graphene oxide [9], carbon nanotubes [10], prussian blue nanoparticles [11], carbon nanodots [12] and folate-polyoxometalate hybrid spheres [13] have been reported to possess peroxidase-like activity and used for the visual detection of H_2O_2 and glucose. In recent years, mesoporous silica nanoparticles (MSN) have gained great interests in many fields due to their unique advantages, including good biocompatibility, large load capacity, tunable pore sizes, the ease of surface functionalization, large surface area, and high thermal and mechanical stability [14–17]. More importantly, MSN can encapsulate or immobilize a large amount of payloads such as mediators, enzymes, and antibodies owning to their high pore volume and large surface area [18,19]. Moreover, the surface properties and composition of MSN can be easily tailored by changing the organic components during the MSN preparation process, which makes them considerably attractive for a wide arrange of applications such as catalyst, drug release, sensors and separation [20,21].

In this work, we synthesized a type of Fe_3O_4@MSN with Fe_3O_4 as the core and mesoporous silica the shell. The superparamagnetic Fe_3O_4 core provides high peroxidase-mimic activity and makes artificial enzymatic system easily recyclable. Furthermore, Fe_3O_4 nanoparticles are encapsulated in MSN shells to hinder the aggregation and keep them stable even under harsh conditions. Meanwhile, small active molecules are allowed to diffuse in and out of the MSN shells. Serving as robust nanoreactors, the Fe_3O_4@MSN can catalyze a self-organized cascade reaction based on these functional units mentioned above, namely oxidation of glucose by oxygen to yield gluconic acid and H_2O_2 in the first place, and sequently the H_2O_2

* Corresponding author.
E-mail addresses: bionano@163.com (Y. Wang), kmwang@hnu.edu.cn (K. Wang).

http://dx.doi.org/10.1016/j.talanta.2014.12.013
0039-9140/

further oxidizes 3,3,5,5-tetramethylbenzidine (TMB) to produce a color change. It is known to all that Fe_3O_4@MSN was used successfully for hydrogen peroxide and glucose detection for the first time. And the catalytic efficiency of Fe_3O_4@MSN was not strongly dependent on pH and temperature. As a nanoreactor, Fe_3O_4@MSN can catalyze a self-organized cascade reaction and simultaneously optimized the test with a better sensitivity while MSN is comparatively conceivable to be modified in the application of interface detection.

2. Experimental section

2.1. Chemicals and materials

Tetraethylorthosilicate (TEOS), cetyltrimethylammonium bromide (CTAB), glucose oxidase (GOx), horseradish peroxidase (HRP), 3, 3, 5, 5-tetramethylbenzidine (TMB) were purchased from Sigma-Aldrich. Glucose, fructose, maltose and lactose were obtained from Shanghai Sangon Biological Engineering Technology and Service Co. Ltd., China. $FeCl_3$•6 H_2O, sodium acetate, ethylene glycol, ethylenediamine and 30% hydrogen peroxide (H_2O_2) were purchased from Beijing Chemical Reagent Company (Beijing, China). Other reagents and chemicals were at least analytical reagent grade. All materials were purchased and used as received without further treatment. The water used throughout all experiments was purified by a Milli-Q system (18.2 MΩ-cm, Millipore System Inc.).

2.2. Synthesis of magnetite core

The spherical magnetic Fe_3O_4 particles were prepared according to the literature [22,23]. Typically, $FeCl_3$•6 H_2O (0.5 g) and sodium acetate (1.5 g) were quickly added into a mixed solution of ethylene glycol (10 mL) and ethylenediamine (5 mL). After vigorously stirring for 30 min, the obtained solution was transferred to a Teflon-lined stainless-steel autoclave and heated at 200 °C for 24 h. The autoclave was then cooled to room temperature naturally. The obtained black magnetite particles were washed with ethanol and deionized water in sequence, and dried in hot air oven at 80 °C for 24 h.

2.3. Synthesis of Fe_3O_4@MSN nanocomposites

The core–shell structured Fe_3O_4@ MSN nanocomposites were prepared by the modified Stöber sol–gel method [24]. In a typical procedure, as-prepared Fe_3O_4 (0.10 g) nanoparticles were treated with ethanol by ultrasonication for 30 min. Subsequently, the treated nanoparticles were separated by centrifugation, and then well dispersed in a mixture of ethanol (80 mL), deionized water (20 mL), and concentrated ammonia aqueous solution (28 wt%, 1.0 mL). TEOS (30 μL) was then added dropwise to the solution. After stirring for 6 h, the products were separated by a magnet and washed with ethanol and water, and then redispersed in a mixed solution containing CTAB (0.3 g), deionized water (80 mL), concentrated ammonia aqueous solution (28 wt%, 1.5 mL), and ethanol (60 mL). The resulting solution was vigorously stirred for 30 min. TEOS (400 μL) was then added dropwise to the solution with stirring. After another stirring for 6 h, the products were collected and separated with a magnet, washed with ethanol and water several times to remove the unreacted species, and dried in vacuum at 60 °C for 24 h. Finally, the CTAB-removed product was dried in vacuum at 60 °C for 12 h and denoted as Fe_3O_4@MSN nanocomposites.

2.4. Characterization of Fe_3O_4@MSN nanocomposites

UV–vis absorption spectra were measured on a Beckman DU-800 UV–vis spectrophotometer. The morphology and microstructure of Fe_3O_4@MSN nanocomposites were characterized by using JEM-3010 transmission electron microscopy (TEM) and JSM-6700F scanning electron microscopy (SEM). TEM sample was prepared by applying diluted particle suspensions to formvar film-coated copper grids followed by drying preparations at room temperature. N_2 adsorption-desorption isotherms were obtained at −196 °C on a Micromeritics ASAP 2010 sorptometer by static adsorption procedures. Specific surface areas were calculated from the adsorption data in the low-pressure range using the Brunauer–Emmett–Teller (BET) model. Pore size was calculated by using the Barrett–Joyner–Halenda (BJH) model on the adsorption branch of the isotherm.

2.5. H_2O_2 detection using Fe_3O_4@MSN as peroxidase mimetics

To investigate the peroxidase-like activity of the as-prepared Fe_3O_4@MSN, the catalytic oxidation of the peroxidase substrate TMB in the presence of H_2O_2 was tested. In a typical experiment, 30 μL of 60 mM TMB, 25 μL of the Fe_3O_4@MSN stock solution, and 30 μL of 100 mM H_2O_2 were added into 115 μL of 0.2 M acetate buffer, the mixed solution was incubated for 20 min. The Fe_3O_4@MSN was then removed from the reaction solution by an external magnetic field. 100 μL of the resulting reaction solution was used for absorption spectroscopy measurement. To examine the influence of reaction buffer pH on the Fe_3O_4@MSN activity, 0.1 M acetate buffer solutions from pH 2.0 to 12.0 were investigated. To examine the influence of incubation temperature on the Fe_3O_4@MSN activity, catalytic reactions incubated in different temperature water baths from 20 to 80 °C were investigated. As control experiments, 10 μL of water was used instead of 10 mL of Fe_3O_4@MSN.

2.6. Glucose detection using Fe_3O_4@MSN

Glucose detection was realized as follows: (1) 20 μL of 20 mg/mL GOx and 80 μL of glucose of different concentrations in 10 mM phosphate buffered saline (PBS, pH 7.4) were incubated for 20 min; (2) 30 μL of 60 mM TMB, 25 μL of the Fe_3O_4@MSN stock solution, and 845 μL of 0.2 M acetate buffer (pH 5.5) were added into the above 100 μL glucose reaction solution; (3) the mixed solution was incubated in a 40 °C water bath for 20 min, and the Fe_3O_4@MSN were then removed from the reaction solution by an external magnetic field; (4) the final reaction solution was used to perform the absorption spectroscopy measurement. In control experiments, 5 mM maltose, 5 mM lactose, and 5 mM fructose were used instead of glucose.

3. Results and discussion

3.1. Characterization of Fe_3O_4@MSN

The SEM and TEM were used to characterize the synthesized Fe_3O_4@MSN nanoparticles. The SEM and TEM micrograph of Fe_3O_4@MSN are displayed in Fig. 1. One can see that the size distribution of Fe_3O_4@MSN with an average diameter and length of ~100 nm. The magnetic core inside the mesoporous silica matrix is loose clusters composed of nanocrystals. As can be seen from Fig. 2A, the black solution was Fe_3O_4@MSN nanocomposites (photo a), and precipitate could be observed in the aqueous medium and the supernatant of the aqueous medium became transparent after magnetic treatment (photo b). Additionally, the N_2 adsorption-desorption isotherms of Fe_3O_4@MSN showed a typical MCM-41 structure (type IV) with a BET surface area of 506.18 $m^2\ g^{-1}$. The BJH curve showed narrow pore size distribution of Fe_3O_4@MSN with an average pore diameter of 2.4 nm and pore volume of 0.86 $cm^3\ g^{-1}$ (Fig. 2B). These findings provided immediate evidence for the fact that Fe_3O_4@MSN nanocomposites were synthesized.

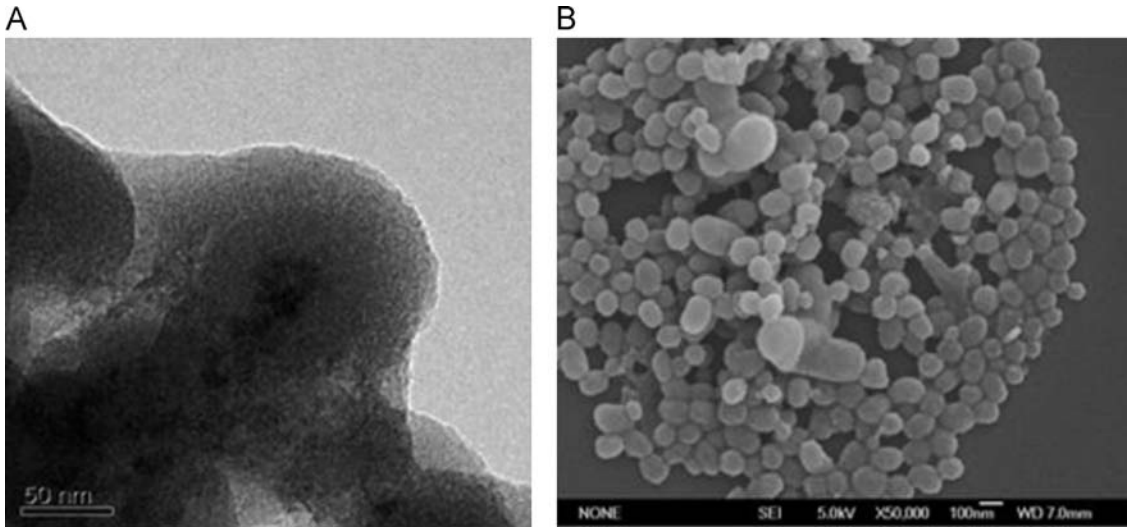

Fig. 1. Characterization of synthesized Fe_3O_4@MSN. (A) TEM image of Fe_3O_4@MSN; and (B) SEM image of Fe_3O_4@MSN.

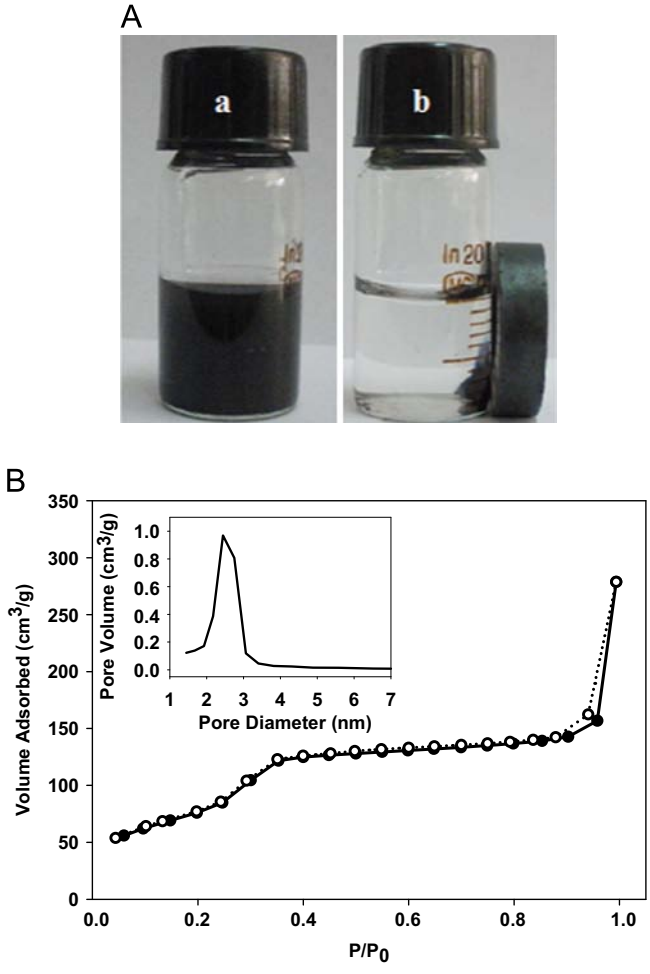

Fig. 2. (A) Photographs of Fe_3O_4@MSN in pH 5.5 buffers without (a) and with (b) magnetic treatment; (B) Nitrogen adsorption-desorption isotherms and pore size distribution of Fe_3O_4@MSN (inset).

3.2. The Fe_3O_4@MSN as peroxidase mimetics and their use in H_2O_2 detection

It is well known that peroxidase can catalyze the oxidation of peroxidase substrate by hydrogen peroxide to produce a color change [25]. To investigate the peroxidase-like activity of the as-prepared Fe_3O_4@MSN, the catalytic oxidation of peroxidase substrate TMB in the presence of H_2O_2 was tested (Eq. (1)). Because the amount of the colored oxidized TMB product is proportional to the concentration of H_2O_2 present in the solution, the concentration of H_2O_2 can be determined by recording the absorbance of the solution according to the Beer's law. As seen in Fig. 3A, upon the addition of Fe_3O_4@MSN to the peroxidase substrate TMB in the presence of H_2O_2, a blue color product can be formed. And the blue color of the solution results from the product formed by the oxidation of TMB. The resulting solution shows a maximum absorbance at 655 nm in the UV–vis spectrum originates from the oxidation of TMB (Fig. 3B), indicating that Fe_3O_4@MSN has peroxidase-like catalytic activity in the absence of any other catalysts [26,27].

$$H_2O_2 + TMB \xrightarrow{Fe_3O_4@MSN} 2H_2O + oxidized\ TMB \quad (1)$$

Similar to peroxidase, the catalytic activity of Fe_3O_4 dependent on solution pH and reaction temperature has been reported [1], but the pH and temperature-dependent activity of Fe_3O_4@MSN remains unknown, which was therefore also investigated in this study. And the result indicates that the activity of Fe_3O_4@MSN is not strongly dependent on solution pH and reaction temperature. In view of the stability and catalytic activity of the Fe_3O_4@MSN, 40 °C was taken as the optimal reaction temperature and pH 5.5 was set as the optimal pH value. Because the catalytic activity of the Fe_3O_4@MSN is H_2O_2 concentration-dependent, the system discussed above could be used to detect H_2O_2. Under the optimal conditions, the developed method was used for H_2O_2 detection. Fig. 4A shows a typical H_2O_2 concentration response curve. The calibration graph of the absorbance at 655 nm to H_2O_2 concentration was linear in the range from 1.0×10^{-6} to 1.0×10^{-4} mol/L where as low as 1.0×10^{-6} mol/L H_2O_2 could be detected under the optimal experimental conditions (Fig. 4B). The regression equation was $y=0.0287x+0.2685$ (y is the absorption values, x is H_2O_2 concentration) and the correlation coefficient was 0.9852.

3.3. The stability of Fe_3O_4@MSN catalytic activity

In general, the activity of natural enzyme is lost after exposure to extremes of pH and high temperature. As for horseradish peroxidase, after treatment at $<$ pH 5.5 or $>$ temperatures 40 °C for only 2 h, the enzyme activity dramatically declined. In contrast, Fe_3O_4@MSN is

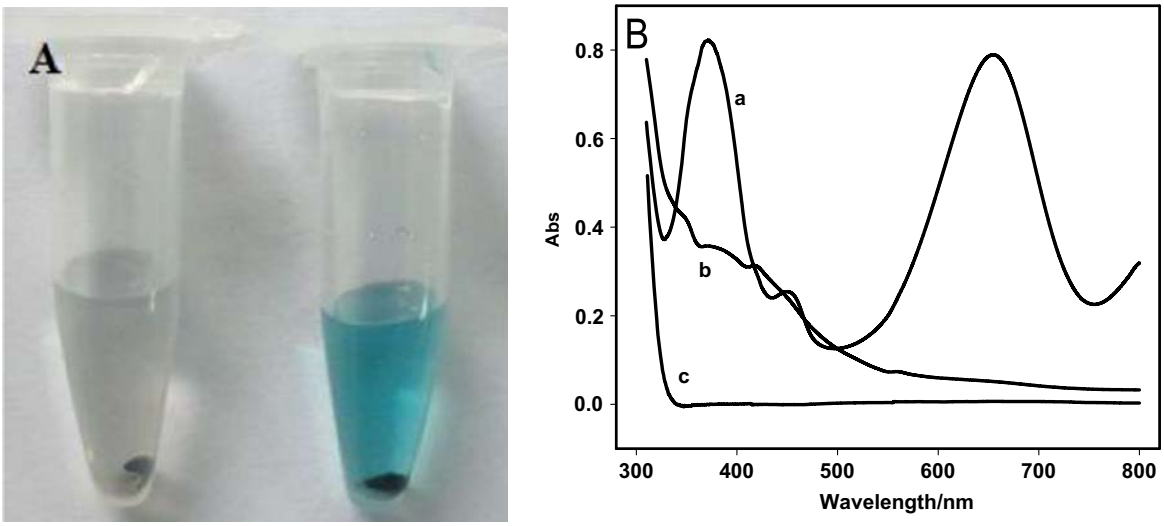

Fig. 3. (A) Typical photographs of TMB catalytically oxidized by the Fe_3O_4@MSN in the absence (left) and in the presence of H_2O_2 (right). (B) Absorption curves of TMB reaction solutions catalytically oxidized by the as-prepared Fe_3O_4@MSN in the presence of H_2O_2 incubated at 40 °C in pH 5.5 buffers (line a. TMB + Fe_3O_4@MSN + H_2O_2, line b. TMB + H_2O_2, line c. Fe_3O_4@MSN + H_2O_2).

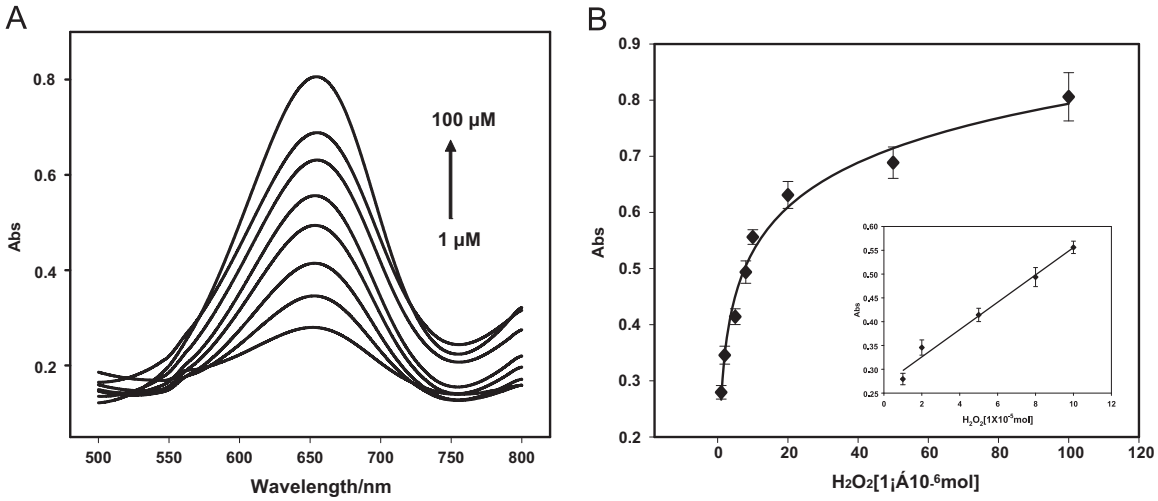

Fig. 4. (A) A dose response curve for H_2O_2 detection using the as-prepared Fe_3O_4@MSN as artificial enzymes and (B) the Linear calibration plot between the absorbance at 655 nm and concentration of H_2O_2 (0.01 mM to 1 mM). The error bars represent the standard deviation of three measurements. The insert shows the dependence of the absorbance at 655 nm on the concentration of H_2O_2 in the range 1 μM to 10 μM.

expected to be more stable because it is an inorganic material. To verify this, the catalytic activity of Fe_3O_4@MSN was measured after incubation at a range of temperatures and pH values. The experimental results show that the Fe_3O_4@MSN are indeed stable over a wide range of pH from 2.0 to 12.0, and temperature from 40 to 90 °C. The study on the Fe_3O_4@MSN catalytic activity suggests that the reproducibility of Fe_3O_4@MSN samples prepared at different times is satisfactory (the relative catalytic activity of the Fe_3O_4@MSN could retain more than its 95% original value after used for 5 times.) (Fig. 5). The robustness of Fe_3O_4@MSN makes them suitable for a broad range of applications in the biomedicine and environmental chemistry fields.

3.4. Glucose detection using GOx and the Fe_3O_4@MSN

H_2O_2 is the main product of glucose oxidase-catalyzed reaction. When the peroxidase-like activity of the Fe_3O_4@MSN is coupled with the glucose catalytic reaction by GOx, colorimetric determination of glucose could be realized. The GO*x* oxidizes glucose to form gluconic acid and H_2O_2 quantitatively, and the H_2O_2 produced is then utilized by Fe_3O_4@MSN to oxidize TMB to produce a blue colored solution (Eq. (2)). Therefore, colorimetric detection of glucose could be easily realized using the colorimetric method. By this methodology, the calibration graph of the absorbance at 655 nm to concentration of glucose was found to be linear in the range 1.0×10^{-5} to 5.0×10^{-4} mol/L with a correlation coefficient of 0.9958 (Fig. 6) The regression equation was $y = 0.0273x + 0.2452$ (y is the absorption value, x is the glucose concentration). The detection limit (LOD) was 0.4×10^{-5} mol/L calculated according to the signal which is equivalent to 3 times the standard deviation of the blanks.

$$O_2 + glucose \xrightarrow{GOx\ H_2O_2} + gluconic\ acid \quad (2)$$

Most of the Fe_3O_4@MSN catalysts are anchored inside the pore channels that give accesses to small molecules such as H_2O_2 and TMB while obstruct large molecules like glucose oxidase. As a result, multistep reactions occur at two different parts of the material, namely generation of H_2O_2 from glucose using Fe_3O_4@MSN occurring outside the pore channels while the oxidation of TMB by the Fe_3O_4@MSN inside the pore channels. This allows two different catalytic reactions to proceed simultaneously at two parts of the material without interfering with each other.

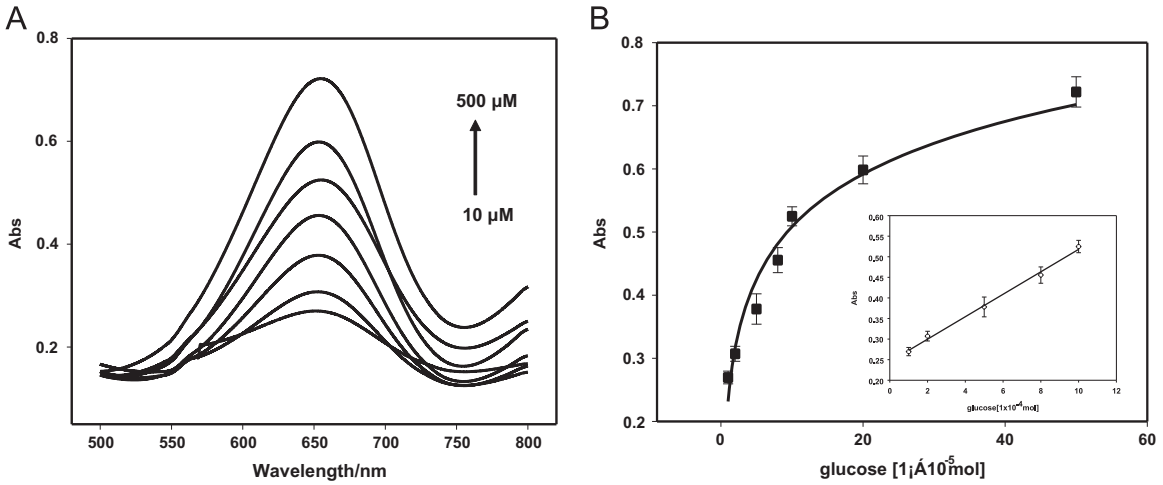

Fig. 5. (A) A dose response curve for glucose detection using the as-prepared Fe_3O_4@MSN as artificial enzymes and (B) the Linear calibration plot between the absorbance at 655 nm and concentration of glucose (10 μM to 500 μM). The error bars represent the standard deviation of three measurements. The insert shows the dependence of the absorbance at 655 nm on the concentration of glucose in the range 10 μM to 100 μM.

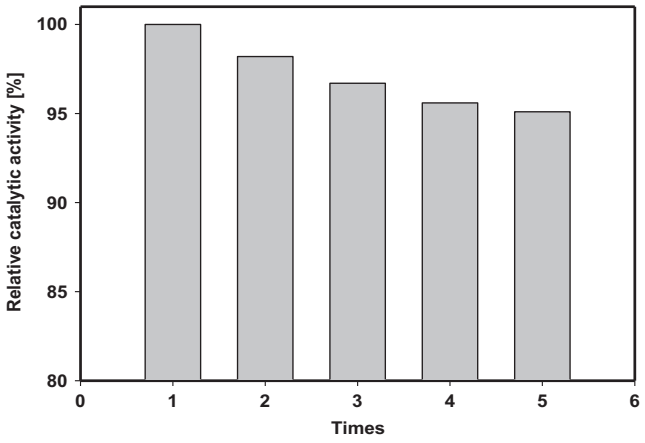

Fig. 6. The relative catalytic activity of Fe_3O_4@MSN after 5 cycles.

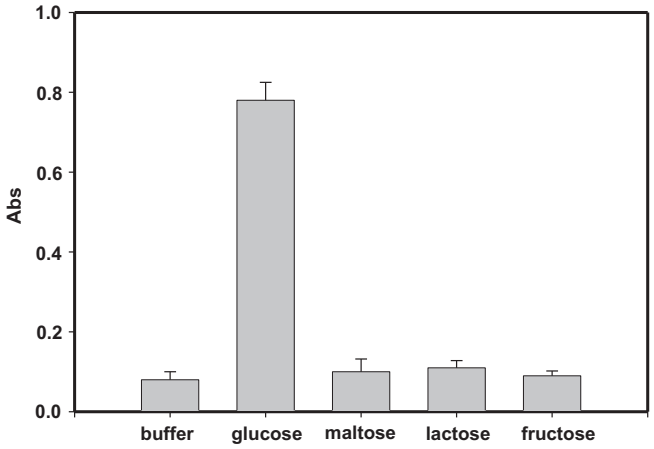

Fig. 7. Determination of the selectivity of glucose detection with 5 mM lactose, 5 mM fructose, 5 mM maltose, and 1 mM glucose using GOD and Fe_3O_4@MSN. The error bars represent the standard deviation of three measurements.

3.5. Study of interference and selectivity

In order to test whether the detection of glucose is specific or not, control experiments were taken using fructose, lactose, and maltose respectively. Before it, however, the selectivity is very important in the real application. For glucose detection, the selectivity experiments were carried out using buffer solution, 5 mM maltose, 5 mM fructose, and 5 mM lactose in place of glucose (5 mM). The results demonstrated that the intensity of these glucose analogs was negligible compared with that of glucose even at concentrations as high as 5 mM (Fig. 7). Thus the method developed here showed high selectivity toward glucose detection. This indicates that this biosensing system has high selectivity for glucose, which could be attributed to the high affinity of glucose oxidase for glucose detection.

4. Conclusion

In summary, Fe_3O_4@MSN were prepared and investigated as peroxidase mimetics. The catalytic oxidation of peroxidase substrate TMB with H_2O_2 using the Fe_3O_4@MSN was realized. The Fe_3O_4@MSN as peroxidase mimetic provides a colorimetric assay for H_2O_2. The colorimetric method showed good response toward H_2O_2 detection with a linear range from 1×10^{-6} to 1×10^{-4} mol/L. More importantly, a sensitive and selective analytical platform for glucose detection was fabricated using GO*x* and the as-prepared Fe_3O_4@MSN. The analytical platform developed exhibited sensitive and selective detection of glucose with the linear range from 1×10^{-5} to 5×10^{-4} mol/L. Because the Fe_3O_4@MSN can rival natural enzymes due to their easy preparation, robustness, and stability in rough conditions, the analytical platform for the detection of H_2O_2 and glucose developed here not only confirms that the Fe_3O_4@MSN possesses an intrinsic peroxidase-like activity but also shows great potential applications in varieties of simple, cost-effective, and easy-to-make biosensors in the future.

Acknowledgments

This work was supported in part by the National Natural Science Foundation of China (21305164), State Key Laboratory of Chemo/Biosensing and Chemometrics, Hunan University (2013019), Scientific Research Fund of Hunan Provincial Education Department (13C1138).

References

[1] L.Z. Gao, J. Zhuang, L. Nie, J.B. Zhang, Y. Zhang, N. Gu, T.H. Wang, J.V. Feng, D.L. Yang, S. Perrett, X.Y. Yan, Nat. Nanotechnol. 2 (2007) 577–583.
[2] H. Wei, E. Wang, Anal. Chem. 80 (2008) 2250–2254.

[3] Y. Shi, P. Su, Y. Wang, Y. Yang, Talanta 130 (2014) 259–264.
[4] Y. Jv, B.X. Li, R. Cao, Chem. Commun. 46 (2010) 8017–8019.
[5] W. Chen, J. Chen, A.L. Liu, L.M. Wang, G.W. Li, X.H. Lin, Chem. Catal. Chem. 3 (2011) 1151–1154.
[6] A.K. Dutta, S. Das, S. Samanta, P.K. Samanta, B. Adhikary, P. Biswas, Talanta 107 (2013) 361–367.
[7] M. Ornatska, E. Sharpe, D. Andreescu, S. Andreescu, Anal. Chem. 83 (2011) 4273–4280.
[8] A. Asati, S. Santra, C. Kaittanis, S. Nath, J.M. Perez, Angew. Chem. Int. Ed. 48 (2009) 2308–2312.
[9] Y. Song, K. Qu, C. Zhao, J. Ren, X. Qu, Adv. Mater. 22 (2010) 2206–2210.
[10] Y. Song, X. Wang, C. Zhao, K. Qu, J. Ren, X. Qu, Chem. Eur. J. 16 (2010) 3617–3621.
[11] W. Zhang, D. Ma, J. Du, Talanta 120 (2014) 362–367.
[12] W. Shi, Q. Wang, Y. Long, Z. Cheng, S. Chen, H. Zheng, Y. Huang, Chem. Commun. 47 (2011) 6695–6697.
[13] J. Wang, X. Mi, H. Guan, X. Wang, Y. Wu, Chem. Commun. 47 (2011) 2940–2942.
[14] E. Climent, M.D. Marcos, R. Martinez-Manez, F. Sancenon, J. Soto, K. Rurack, P. Amoros, Angew. Chem. Int. Ed. 48 (2009) 8519–8522.
[15] W.Y. Cai, I.R. Gentle, G.Q. Lu, J.J. Zhu, A.M. Yu, Anal Chem. 80 (2008) 5401–5406.
[16] I. Slowing, B.G. Trewyn, V.S.Y. Lin, J. Am. Chem. Soc. 128 (2006) 14792–14793.
[17] H. Zhou, S.S. Wu, J. Shen, Chem. Rev. 108 (2008) 3893–3957.
[18] D.R. Radu, C.Y. Lai, J.W. Wiench, M. Pruski, V.S.Y. Lin, J. Am. Chem. Soc. 126 (2004) 1640–1641.
[19] I.I. Slowing, B.G. Trewyn, V.S.Y. Lin, J. Am. Chem. Soc. 129 (2007) 8845–8849.
[20] J.L. Vivero-Escoto, I.I. Slowing, C.W. Wu, V.S.Y. Lin, J. Am. Chem. Soc. 131 (2009) 3462–3463.
[21] V.S.Y. Lin, C.Y. Lai, J.G. Huang, S.A. Song, S. Xu, J. Am. Chem. Soc. 123 (2001) 11510–11511.
[22] W. Zhao, J. Gu, L. Zhang, H. Chen, J. Shi, J. Am. Chem. Soc. 127 (2005) 8916–8917.
[23] X.-L. Zhang, H.-Y. Niu, W.-H. Li, Y.-L. Shi, Y.-Q. Cai, Chem. Commun. 47 (2011) 4454–4456.
[24] D. He, X. He, K. Wang, Y. Zhao, Z. Zou, Langmuir 29 (2013) 5896–5904.
[25] P.D. Josephy, T. Eling, R.P. Mason, J. Biol. Chem. 257 (1982) 3669–3675.
[26] B. Malvi, C. Panda, B.B. Dhar, S.S. Gupta, Chem. Commun. 48 (2012) 5289–5291.
[27] F. Yu, Y. Huang, A.J. Cole, V.C. Yang, Biomaterials 30 (2009) 4716–4722.